INFECTION AND IMMUNITY, Oct. 2009, p. 4621–4630 Vol. 77, No. 10
0019-9567/09/$08.00+0 doi:10.1128/IAI.00415-09

Cytotoxicity and Secretion of Gamma Interferon Are Carried Out by Distinct CD8 T Cells during *Mycobacterium tuberculosis* Infection▽†

Thorbjorg Einarsdottir, Euan Lockhart, and JoAnne L. Flynn*

Department of Microbiology and Molecular Genetics, University of Pittsburgh School of Medicine, Pittsburgh, Pennsylvania 15261

Received 14 April 2009/Returned for modification 6 July 2009/Accepted 23 July 2009

The host immune response is generally sufficient to contain *Mycobacterium tuberculosis* infection. It does not, however, efficiently prevent subsequent infection with *M. tuberculosis* or provide sterilizing immunity. While the understanding of the immune response generated against this pathogen is incomplete, improvements have been achieved due to advances in immunological tools. In this study, we analyzed the multifunctional nature of primary and memory CD8 T-cell responses generated during murine *M. tuberculosis* infection. We generated a recombinant *M. tuberculosis* strain expressing ovalbumin (OVA) epitopes in order to expand the peptides for the detection of CD8 T cells during *M. tuberculosis* infection and enable us to use OVA-specific reagents. Our results indicate that the majority of *M. tuberculosis*-specific CD8 T cells are limited to either cytotoxicity or the secretion of gamma interferon (IFN-γ), with cytotoxicity being far more prevalent than IFN-γ secretion. Memory CD8 T cells responded earlier and reached higher levels in the lungs than naïve CD8 T cells, as was expected. They were, however, less cytotoxic and secreted less IFN-γ than newly primed CD8 T cells, suggesting that one factor contributing to bacterial persistence and lack of sterilizing immunity may be the low quality of memory cells that are generated.

Mycobacterium tuberculosis, the pathogen causing tuberculosis, is an escalating global health threat that is spread between people by aerosolized droplets. While a subset of people develop primary disease and are infectious, most people contain the infection through a successful immune response. Typing of *M. tuberculosis* strains has shown that people can be infected simultaneously or sequentially with different strains of *M. tuberculosis* (29, 37). Thus, immune responses that are sufficient to contain an initial infection may be unable to prevent the establishment of subsequent *M. tuberculosis* infections. In addition, persons treated for tuberculosis with antimycobacterial drugs can be reinfected and develop disease (36). This is also true in animal models (8, 16, 32). This suggests that memory responses generated during previous mycobacterial infections are not generally capable of protecting against new infections or disease.

It is currently unknown which, if any, immune functions can protect against establishment of infection. In terms of T-cell responses, gamma interferon (IFN-γ) and tumor necrosis factor can activate infected macrophages to induce antimicrobial activity, while cytolysis of infected cells can kill the bacterium or release it to be taken up by healthy cells that are better able to contain it (12, 21). Most studies of the role of CD8 T cells during *M. tuberculosis* infection have focused on either IFN-γ secretion or cytotoxicity. A few studies have examined both functions but not on a single-cell basis (6, 17, 19). These studies indicated that CD8 T-cell-mediated IFN-γ secretion and cytotoxicity peak in the lungs at 4 weeks postinfection. IFN-γ secretion subsequently decreases, while the results differ as to whether cytotoxicity decreases. This difference may be due to variation between mouse strains and epitopes or the techniques used to assess cytotoxicity.

In the current study, we demonstrate that most *M. tuberculosis*-specific CD8 T cells generated during primary infection were limited to either secretion of IFN-γ or cytotoxic function. There was a higher fraction of CD8 T cells with cytotoxic potential compared to those that produced IFN-γ. The CD8 T-cell memory response was similarly exclusive in function. Despite increased degranulation, cells responding during secondary infection were less cytotoxic than cells responding during primary infection. Induction of superior quality CD8 T cells may provide a benefit during *M. tuberculosis* infection, but a more detailed understanding of the complex T-cell response to *M. tuberculosis* is necessary for the development of future preventive and therapeutic strategies.

MATERIALS AND METHODS

***M. tuberculosis* strain ova cloning.** The culture filtrate protein 10 (CFP10) gene (Rv3874; 225 bp) and the 228-bp upstream sequence containing the CFP10 promoter were PCR amplified from *M. tuberculosis* genomic DNA and cloned into the pJL37 cloning vector (5). An 87-bp ovalbumin (OVA) gene fragment containing OT-I- and OT-II-recognized epitopes was PCR amplified from a larger fragment and cloned into pJL37-CFP10. Restriction enzymes (Roche, Indianapolis, IN) and T4 DNA ligase (Invitrogen, Carlsbad, CA) were used, according to the manufacturers' protocols. Plasmids were transformed into DH5α cells (Invitrogen) by a 42°C heat shock for 30 s and purified with the High Pure plasmid isolation kit (Roche), according to the manufacturer's protocols. The CFP10-OVA insert was cloned into the pMH94 integration vector (25) and electroporated (23) into *M. tuberculosis* strain Erdman (originally obtained from the Trudeau Institute, Saranac Lake, NY), using a Gene Pulser II (Bio-Rad, Hercules, CA). pJL37 and pMH94 plasmids were kindly provided by Graham Hatfull.

PCR. AccuPrime (Invitrogen), with primers from Integrated DNA Technologies (Coralville, IA), was used for PCR (95°C [20 s], 45°C [30 s], 68°C [1 min], 32 cycles, 68°C [7 min]), unless otherwise stated.

* Corresponding author. Mailing address: Department of Microbiology and Molecular Genetics, University of Pittsburgh School of Medicine, W1144 Biomedical Science Tower, 200 Lothrop Street, Pittsburgh, PA 15261. Phone: (412) 624-7743. Fax: (412) 648-3394. E-mail: joanne@pitt.edu.

† Supplemental material for this article may be found at http://iai.asm.org/.

▽ Published ahead of print on 10 August 2009.

(i) PCR amplification of CFP10. The primers used for PCR amplification of CFP10 are as follows: CACCTCTAGAGCTCGCGCAGGAGCGTGAAGAAG (sense, CFP10-XbaI 5′) and TATACATATGGAAGCCCATTTGCGAGGAC AGCG (antisense, CFP10-NdeI 3′).

(ii) Primers for PCR amplification of a large OVA fragment. Overlapping primers were designed with the UpGene DNA codon optimization algorithm (13). The primers were annealed and amplified at 94°C (30 s), 52°C (30 s), and 72°C (30 s) for 55 cycles. The primers used are as follows: AACCGGGATCCGGCTCG GAGC (s1), TAATGAATTCTCAGTGATGGT (as1), AGCTGGAGAGCATCA TCAACTTCGAGAAGCTGGGCTCGGAGT (s2), GGTGGTGGTGGCCGCA GGTGGCGAAGTTGTACACGGCCTCG (as2), CGCTGAAGATCTCGCAG GCCGTGCACGCCGCGCACGCCGAGA (s3), AGCCGCGGCCGGCCTCGTT GATCTCGGCGTGCGCGGCGTGCA (as3), TCAACGAGGCCGGCCGCGGC TCGAAGGCCGTGTACAACTTCG (s4), and CGGCCTGCGAGATCTTCA GCGACTCCGAGCCCAGCTTCTCGA (as4).

(iii) Primers for PCR amplification of an 87-bp OVA gene fragment. The primers and sequences used are as follows: CACCCATATGATCTCGCAGGC CGTG (sense, OT-I-NdeI 5′) and GGTGGAATTCGCGGCCGGCCTCGTT (antisense, OT-II-EcoRI 3′).

(iv) PCR amplification for screening and sequencing of CFP10-OVA. The primers used are as follows: CFP10-Xbal 5′ and OT-II-EcoRI 3′ primers (see above). The High Pure PCR product purification kit (Roche) was used, and the product was sequenced at the University of Pittsburgh Sequencing Core Facility (Pittsburgh, PA).

Mice and bacterial infections. Six- to eight-week-old C57BL/6 and B6.SJL-*Ptprc*^{a} *Pepc*^{b}/BoyJ (CD45.1) mice were purchased from Jackson Laboratories (Bar Harbor, ME), while OT-I and OT-II T-cell receptor transgenic mice on a C57BL/6 RAG1$^{-/-}$ background (kindly provided by Louis D. Falo) were bred at the University of Pittsburgh Biotechnology Center (Pittsburgh, PA). Mice were kept under specific pathogen-free conditions in a biosafety level 3 facility. OT-I and OT-II cells were purified from naïve spleens using MACS cell separation technology (Miltenyi, Auburn, CA), according to the manufacturer's protocol. A total of 5×10^3 OT-I and OT-II cells in phosphate-buffered saline (PBS; Sigma, St. Louis, MO) were adoptively transferred to wild-type (WT) C57BL/6 or CD45.1 mice. Twenty-four hours later, the mice were infected with either WT *M. tuberculosis* or *M. tuberculosis* strain ova, using a nose-only exposure aerosolizer (Intox, Moriarty, NM) (2). This delivered approximately 10 to 20 CFU per lung, estimated by plating whole-lung homogenates at 24 h postinfection on 7H10 medium agar (Difco, Sparks, MD) and incubation at 37°C in 5% CO_2 for 3 weeks. A total of 4 to 12 mice were used per time point per experimental procedure. Experiments were performed at least twice. Animal protocols were approved by the University of Pittsburgh Institutional Animal Care and Use Committee.

Antibiotic treatment. For secondary challenge experiments, infected mice were treated for 3 months with 0.1 g/liter isoniazid (Sigma), 0.1 g/liter rifampin (rifampicin) (Sigma), and 8 g/liter pyrazinamide (Acros, Geel, Belgium) in drinking water. Plating of whole-lung homogenates confirmed that no bacteria could be cultured from the lungs after antibiotic treatment.

PD-1 signal blocking treatment. Treatment was initiated during the chronic phase of infection (8 weeks postinfection). Mice were injected intraperitoneally twice a week with anti-PD-1 (200 μg, clone 29F.1A12) and anti-PD-L1 (200 μg, clone 10F.9G2X) antibodies, or with PBS, for 4 weeks. The antibodies were kindly provided by Gordon J. Freeman.

Harvesting of lungs and lymph nodes. Organs were crushed through a 40-μm cell strainer with a 5-ml syringe plunger to obtain single-cell suspensions. An aliquot was used to determine the bacterial load by plating serial dilutions on 7H10 medium agar. For the remainder of the samples, red blood cells were lysed with an NH_4Cl-Tris solution and washed in Dulbecco modified Eagle medium (DMEM; Sigma). Cells were resuspended in T-cell medium (DMEM supplemented with 10% fetal bovine serum [FBS; Sigma], 1 mM Na-pyruvate [Sigma], 2 mM L-glutamine [Invitrogen], 25 mM HEPES [BioWhittaker, Walkersville, MD], and 50 μM 2-mercaptoethanol [Sigma]) and counted based on trypan blue exclusion (Sigma).

ELISPOT assay. Bone marrow-derived dendritic cells (DCs) were used as antigen-presenting cells in enzyme-linked immunospot (ELISPOT) assays. Mouse bone marrow was cultured for 6 days in DMEM supplemented with 10% FBS, 2 mM L-glutamine, 1,000 U/ml granulocyte-macrophage colony-stimulating factor (kindly provided by Binfeng Lu), and 20 ng/ml interleukin-4 (PeproTech, Rocky Hill, NJ). Cells were split, and media were added on day 3. DCs were either left uninfected or infected with *M. tuberculosis* at a multiplicity of infection of 3 for 24 h in media lacking interleukin-4.

ELISPOT plates (MultiScreenHTS 96-well; Millipore, Billerica, MA) were coated with anti-mouse IFN-γ antibody (10 μg/ml, clone R4-6A2) in PBS. A total of 5×10^4 cells were coincubated for 48 h with 4×10^4 DCs. Peptide (4 μg/ml; GAP [GAPINSATAM] or OVA [SIINFEKL]) (GenScript, Piscataway, NJ) was added to DCs to stimulate antigen-specific responses, while *M. tuberculosis*-infected DCs were used to stimulate total *M. tuberculosis*-specific responses. Uninfected DCs and media were used to determine background levels of IFN-γ secretion. Biotinylated anti-mouse IFN-γ antibody (5 μg/ml, clone XMG1.2), streptavidin-conjugated peroxidase (PK6100; Vector Laboratories, Burlingame, CA), and AEC substrate (PK-4200; Vector Laboratories) were used to detect IFN-γ. Spots were counted on an ImmunoSpot automatic ELISPOT reader (Cellular Technology, Shaker Heights, OH).

Flow cytometry. Cells were incubated with GAP (GAPINSATAM) or OVA (SIINFEKL) tetramer-phycoerythrin (Beckman Coulter, Fullerton, CA) for 30 min at 4°C in T-cell medium. The cells were then washed and incubated at 37°C for 5 h in T-cell medium containing 3 μM monensin (Sigma), anti-CD107a and anti-CD107b fluorescein isothiocyanate antibody, anti-CD28 antibody (clone 37.51, 1 μg/ml), and anti-CD3 antibody (clone 145-2C11, 0.1 μg/ml). Cells were then washed, stained with anti-CD8 peridinin chlorophyll protein antibody in 20% mouse serum (Gemini, West Sacramento, CA) in fluorescence-activated cell sorter (FACS) buffer (PBS with 0.1% bovine serum albumin [Sigma] and 0.1% NaN_3 [Sigma]) for 15 min, washed, and fixed in 2% paraformaldehyde (Sigma). Cells were permeabilized in FACS buffer containing 0.2% saponin (Calbiochem, Gibbstown, NJ) and stained with anti-IFN-γ–phycoerythrin–Cy7 and anti-granzyme B-allophycocyanin (Invitrogen). Samples were read on a FACSAria (BD Biosciences, San Jose, CA) and analyzed with FlowJo (Tree Star, Ashland, OR) software. Antibodies were obtained from BD Biosciences, unless otherwise stated.

In vivo cytotoxicity assay. Uninfected splenocytes were labeled with 0.4 mM carboxyfluorescein succinimidyl ester (CFSE^{lo} cells) or 5 mM CFSE (CFSE^{hi} cells) (Molecular Probes, Eugene, OR) for 15 min at 37°C. The reaction was quenched with T-cell medium, and cells were washed in 20% FBS in PBS. CFSE^{lo} cells were pulsed for 1 h with 20 μg/ml peptide in PBS (GAP or OVA used for antigen-specific killing and amino acids 33 to 41 of the lymphocytic choriomeningitis virus [LCMV] glycoprotein used as controls).

CFSE^{hi} and CFSE^{lo} cells were mixed in a 1:1 ratio, and approximately 5×10^7 cells were injected into the tail veins of mice (four mice/group/time point). Mice were sacrificed 18 h later, and cell homogenates were harvested from the lungs and lymph nodes. Cells were washed in FACS buffer and fixed in 4% paraformaldehyde. Samples were read with FACSCalibur (BD Biosciences) and analyzed with FlowJo software. Peptide-specific lysis was measured by the loss of CFSE^{lo} cells compared to that of CFSE^{hi} cells (ratio averaged per group), as follows: percent peptide-specific lysis = $100 - 100 \times$ [(percent CFSE^{lo}/percent CFSE^{hi}) from GAP or OVA group/(percent CFSE^{lo}/percent CFSE^{hi}) from LCMV group].

Statistical analysis. GraphPad Prism 4.01 (GraphPad Software, La Jolla, CA) was used for graphing and statistical analysis. Unpaired, two-sided *t* tests were used for two-group analysis, while two-sided, nonparametric Spearman rank correlation coefficient tests were used to determine correlation. *P* values of <0.05 and 0.01 were considered significant and highly significant, respectively.

RESULTS

Generation of the *M. tuberculosis* ova strain for analysis of the CD8 T-cell response. A scarcity of known *M. tuberculosis*-specific CD8 T-cell immunodominant epitopes in C57BL/6 mice (28) led us to generate a recombinant *M. tuberculosis* strain (ova) expressing OVA epitopes fused to CFP10. CFP10 is a small protein that forms a heterodimer with 6-kDa early secreted antigenic target (ESAT-6), and together they are secreted by *M. tuberculosis* (27). CFP10 epitopes are not efficiently presented by major histocompatibility complex class I molecules in C57BL/6 mice and, thus, do not induce CD8 T-cell responses (19). However, CFP10 elicits robust CD8 T-cell responses in humans (26), nonhuman primates (7, 22), and the C3H mouse strain (19), indicating that CFP10 has access to the antigen presentation pathway. For this reason, CFP10 was chosen as a carrier protein for the OVA epitopes. This construct enables us to take advantage of the numerous OVA-specific immunologic reagents available as well as to compare

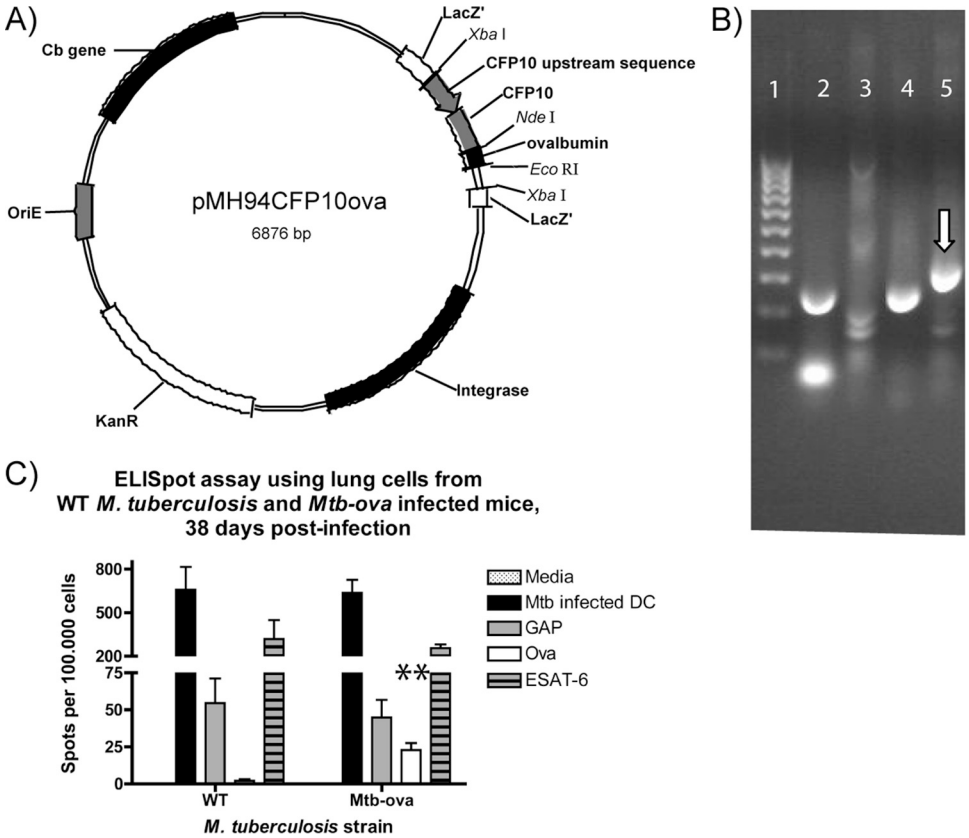

FIG. 1. Generation and screening of *M. tuberculosis* strain ova. (A) Map of pMH94CFP10ova integration vector, drawn with Vector NTI suite 8 (InforMax, Inc.). CFP10 and the upstream sequence were inserted into pMH94, followed by the OVA sequence. The plasmid lacks an origin of replication in *M. tuberculosis* and is lost unless it is integrated in a site-specific manner into the genome by the integrase via the *attP* site. Recombinant colonies were selected based on kanamycin resistance (KanR). (B) PCR screening for integration of pMH94CFP10ova into *M. tuberculosis*. Lane 1 shows a 100-bp DNA ladder (Invitrogen). Lanes 2 (WT *M. tuberculosis*) and 4 (*M. tuberculosis* strain ova) show positive controls, screening for endogenous copies of CFP10 (225 bp). Lanes 3 (WT *M. tuberculosis*) and 5 (*M. tuberculosis* strain ova) screen for pMH94CFP10ova, with primers specific for the ends of the CFP10-OVA fusion gene (312 bp; indicated by the arrow). The figure has been edited to remove irrelevant lanes. (C) ELISPOT assay measuring IFN-γ secretion in response to *M. tuberculosis* (Mtb), endogenous T-cell epitopes (GAP and ESAT-6), OVA CD8 T-cell epitopes, and background levels (media). The data are the means ± standard errors of means from testing results for four mice. OVA-specific CD8 T-cell responses induced by *M. tuberculosis* strain ova (Mtb-ova) were statistically different (**, $P < 0.01$) than responses induced by WT *M. tuberculosis*, while other responses were not statistically different.

OVA-specific responses in the context of *M. tuberculosis* infection to those in other infections where recombinant OVA-expressing strains have been used. Here, we used this construct to compare responses to the following two different CD8 T-cell epitopes: OVA and an endogenous *M. tuberculosis* CD8 T-cell epitope (GAPINSATAM, designated GAP, from Rv0125 [15]).

OVA epitopes 257 to 264 (SIINFEKL) and 323 to 339 (ISQAVHAAHAEINEAGR) are recognized by *H-2*^{b}-restricted OT-I transgenic CD8 T cells and I-A^b-restricted OT-II transgenic CD4 T cells, respectively (14), as well as nontransgenic T cells in C57BL/6 mice. *M. tuberculosis* strain ova was generated by fusing OT-I- and OT-II-recognized sequences downstream of the intact CFP10 gene and upstream regulatory sequences. The CFP10-OVA fusion gene was inserted into pMH94, a vector that integrates into the bacterial genome (25) (Fig. 1A and B). Integration of the pMH94CFP10ova plasmid did not alter the growth rate or survival of the bacterium in vitro or in vivo compared to the parent *M. tuberculosis* Erdman strain (data not shown). *M. tuberculosis* ova, but not WT *M. tuberculosis*, induced OVA-specific responses, as demonstrated by IFN-γ ELISPOT assay ($P < 0.01$) (Fig. 1C). OVA-specific CD4 T-cell responses were always weaker than OVA-specific CD8 T-cell responses. Endogenous T-cell responses to GAP (CD8) and ESAT-6 peptide amino acids 1 to 20 (CD4) were not altered by the plasmid integration, nor were any differences in the outcomes of mice inoculated with *M. tuberculosis* strain ova and WT *M. tuberculosis* observed. In summary, we generated a recombinant *M. tuberculosis* strain expressing OVA epitopes, expanding the repertoire of peptides for the detection of CD8 T cells during *M. tuberculosis* infection.

Expansion of CD8 T cells specific for GAP and OVA during primary infection with *M. tuberculosis* strain ova. In C57BL/6 mice infected by aerosol with a low dose of *M. tuberculosis*, primary T-cell responses can be detected 2 to 3 weeks postinfection. We used tetramers to quantify GAP- and OVA-specific populations of CD8 T cells. In infected mice, GAP- and OVA-specific CD8 T cells comprised about 2 to 10% of the primary CD8 T-cell response in the lungs and 1 to 13% in the lymph nodes (see Fig. S1A and B in the supplemental mate-

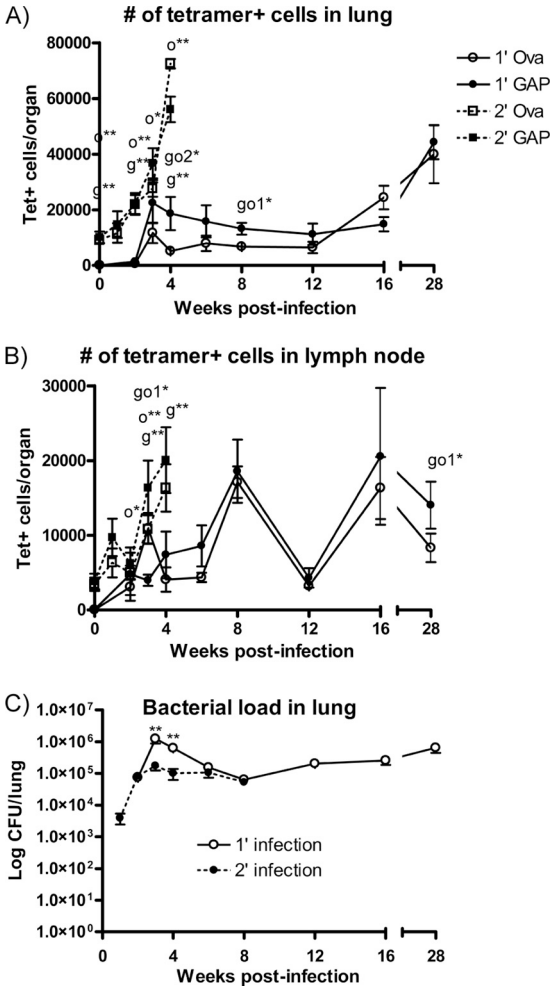

FIG. 2. *M. tuberculosis* strain ova induces similar GAP- and OVA-specific responses. Based on the percent tetramer-positive (Tet^+) CD8 T cells (see Fig. S1A and B in the supplemental material) and live cell numbers (data not shown), the numbers of tetramer-positive cells in the lungs (A) and lymph nodes (B) were calculated. The frequencies of tetramer-specific cells during primary (1′) and secondary (2′) infections were significantly different at 0, 2, 3, and 4 weeks postinfection for OVA-specific cells (o*) and at 0, 2, and 4 weeks postinfection for GAP-specific cells (g*). The frequencies of OVA- and GAP-specific cells were significantly different at 8 weeks (lungs) and 28 weeks (lymph nodes) after primary infection (go1*) and 4 weeks (lungs) after secondary infection (go2*). (C) Bacterial load in the lungs. Primary and secondary infections were statistically different at 3 and 4 weeks postinfection ($P < 0.01$). Data are the means ± standard errors of the means from test results for 4 (A and B) to 12 (C) mice per time point.

rial). This response was sustained for at least 7 months postinfection. GAP- and OVA-specific CD8 T-cell responses were similar, peaking first at 3 weeks postinfection and then contracting as bacterial expansion was controlled (Fig. 2A to C) (24). GAP- and OVA-specific CD8 T cells expanded again late in infection in the lung, which was associated with an increase in the bacterial load ($P < 0.05$, week 16 versus week 28 postinfection) (Fig. 2C). CD8 T-cell expansion late in infection was observed previously (24).

In summary, GAP and OVA induced similar primary CD8 T-cell expansions, which were detected in both acute and chronic phases of infection in the lung and, to a lesser extent, in the mediastinal lymph nodes.

GAP- and OVA-specific CD8 T-cell function during primary infection. To characterize the effector functions of individual *M. tuberculosis*-specific CD8 T cells over the course of infection, we examined CD8 T-cell-mediated cytotoxicity and cytokine production on a single-cell basis using flow cytometry. For this, we used intracellular cytokine staining for IFN-γ and surface staining for CD107 (see Fig. S2A in the supplemental material). CD107a and CD107b are lysosomal proteins that are transiently exposed to the surface upon degranulation, which is indicative of cytotoxicity (4). Incubation of the cells with anti-CD107 antibody during stimulation provides an assay to assess which cells were degranulated during the incubation period.

Two weeks postinfection, GAP- and OVA-specific CD8 T cells started expanding in the lymph nodes (Fig. 2B); by 3 weeks postinfection, primed GAP- and OVA-specific CD8 T cells had expanded and migrated to the lungs (Fig. 2A). By 3 weeks postinfection, 25% of GAP- and OVA-specific CD8 T cells in the lungs had acquired the ability to be cytotoxic (i.e., $CD107^+$), while little degranulation was detected in the lymph nodes (see Fig. S3A and B and S4A and B in the supplemental material). Approximately 15% of GAP- and OVA-specific CD8 T cells in both the lungs and lymph nodes acquired the ability to secrete IFN-γ. Less than 5% of the cells were able to both degranulate and secrete IFN-γ, indicating that distinct populations of cells carry out these functions.

By 4 weeks postinfection, there was an increase in the frequency and number of cytotoxic cells in the lungs, while there were fewer IFN-γ-secreting cells (Fig. 3A and B). However, IFN-γ production peaked at 4 weeks postinfection, as measured by ELISPOT assay using *M. tuberculosis*-infected DCs (see Fig. S5 in the supplemental material) or peptide-pulsed DCs as stimulators (Fig. 4A). The difference in the results is likely due to the following differences in the methods: ELISPOT assay includes stimulation by antigen-pulsed or infected DCs for 2 days, while intracellular cytokine staining occurs during a short (5-h) stimulation with tetramer and anti-CD3/CD28 antibody. The longer stimulation may induce production of IFN-γ from cells that are not immediately ready to produce it. There may also be differences in the sensitivity of the assays (20).

In vivo cytotoxicity assays (Fig. 4B) showed a peak in cytotoxic activity against GAP- and OVA peptide-loaded cells in the lungs at 4 weeks postinfection. Cytotoxicity decreased after the 4-week peak but then slowly increased during the chronic phase of infection. Comparison of the pattern of GAP-specific cytotoxicity and the frequency of $CD107^+$ GAP-specific cells in lungs over the course of infection (Fig. 4C) supports the idea that CD107 surface expression is a good indicator of cytotoxicity during primary *M. tuberculosis* infection.

By 7 months postinfection, expansion of $CD107^+$ and IFN-γ^+ $CD107^+$ T cells was observed (Fig. 3A and B; see also Fig. S3A and B and S4A and B in the supplemental material). These data indicate a dynamic response to *M. tuberculosis* over the acute and chronic phases of infection, with changes in the effector functions of CD8 T cells. However, the assays are not able to discriminate whether cellular function changes over time or whether new cells appear with different functions.

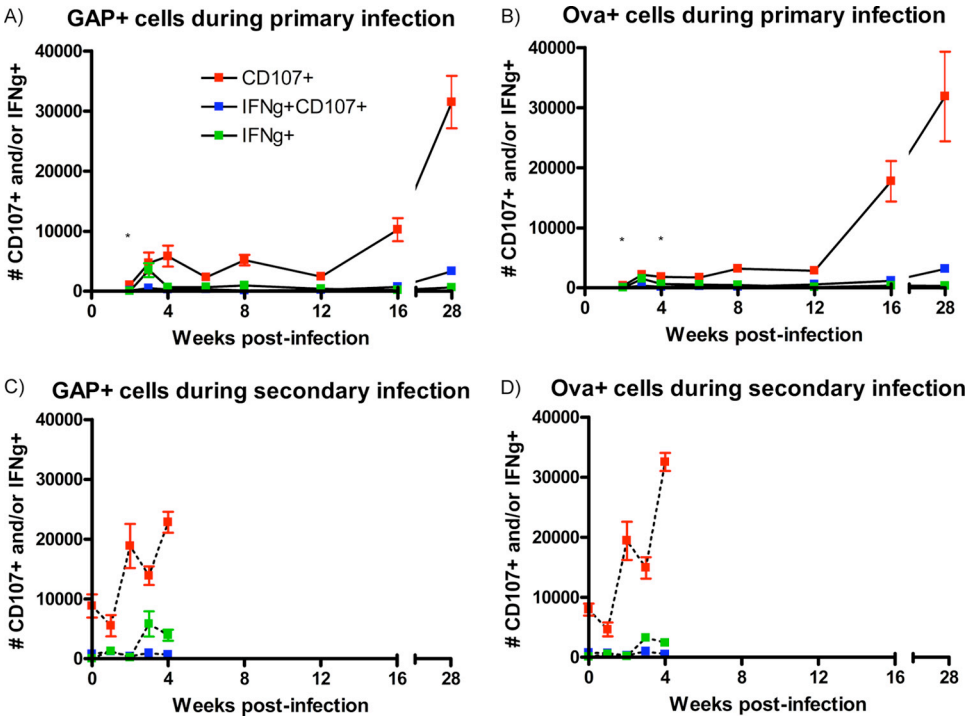

FIG. 3. IFN-γ secretion and degranulation are carried out by distinct populations of cells. Based on GAP- and OVA-specific CD8 T-cell numbers shown in Fig. 2A and percent IFN-γ^+ (IFNg$^+$) and CD107$^+$ cells (see Fig. S3A and B in the supplemental material), numbers of cells per organ were calculated for primary (A and B) and secondary (C and D) infections. (A and C) GAP; (B and D) OVA. The data are the means ± standard errors of the means from test results for four mice per time point. There was a significant difference in the frequency ($P < 0.05$) and number ($P < 0.05$) of IFN-γ^+ CD107$^+$ cells between primary and secondary infections for GAP-specific cells at 2 weeks postinfection and OVA-specific CD8 T cells at 2 and 4 weeks postinfection.

In summary, cells primed in the lymph nodes primarily secreted IFN-γ but lost the ability to secrete IFN-γ after the first month of infection and later acquired cytotoxic function. Effector cells migrating to the lungs retained the phenotype expressed in the lymph nodes or acquired cytotoxic function. Again, IFN-γ was mostly lost after the first month of infection. Cytotoxicity and secretion of IFN-γ were carried out by distinct cell populations.

Blocking PD-1 signaling during primary infection. PD-1 is a negative costimulatory molecule, whose expression is upregulated following T-cell activation (3). A high expression level of PD-1 has been implicated in CD8 T-cell exhaustion in several chronic infections in humans, e.g., human immunodeficiency virus (11, 31) and hepatitis C virus (34), as well as in animal models, e.g., LCMV (3). Using congenic strain differences, we examined temporal expression of PD-1 by adoptively transferring CD45.2 OT-I T cells into CD45.1 background mice. The frequency of *M. tuberculosis*-specific cells expressing PD-1 increased in both the lungs and lymph nodes following infection and continued to increase as infection progressed (Fig. 5A). Mean fluorescence intensity (MFI), however, was highest immediately upon priming, after which PD-1 levels remained low (Fig. 5B; see also Fig. S2G and H in the supplemental material).

The administration of PD-1-blocking antibody during chronic infections (3, 11, 31, 34) has been shown to improve CD8 T-cell function and lower viral loads. Thus, we examined whether intraperitoneal administration of blocking antibodies against PD-1 and PD-L1 would significantly alter CD8 T-cell function, specifically the ability of CD8 T cells to make IFN-γ and be cytotoxic. Treatment was initiated 8 weeks postinfection, which we define as the beginning of chronic phase, and was continued over a 4-week period. This treatment did not produce cells capable of both being cytotoxic and secreting IFN-γ (Fig. 5C; see also Fig. S2D in the supplemental material), indicating that PD-1 is not involved in maintaining the functional distinction of cytotoxic cells and cells that secrete IFN-γ. Treatment did not significantly alter the frequency of CD107$^+$ and IFN-γ^+ cells or the bacterial load (Fig. 5D).

In summary, while the frequency of PD-1-expressing cells increased with time, expression levels on a per-cell basis decreased, indicating that newly primed cells expressed PD-1 and that its expression then decreased. Blocking PD-1 signaling had no appreciable effect on CD8 T-cell function, as measured here. It is possible that blocking PD1 signaling at a different time point, either earlier or later in infection, may affect CD8 T-cell function.

Expansion of CD8 T cells specific for GAP and OVA epitopes during rechallenge with *M. tuberculosis* strain ova. As a model for studying memory responses, mice were infected with *M. tuberculosis* for 2 months and then treated with antibiotics in drinking water for 3 months, after which no bacteria could be cultured from whole-lung homogenates. Mice were then reinfected and sacrificed at weekly time points. Recalled memory T cells can be examined for the first 2 weeks postinfection. After that time, the response is likely to consist of both

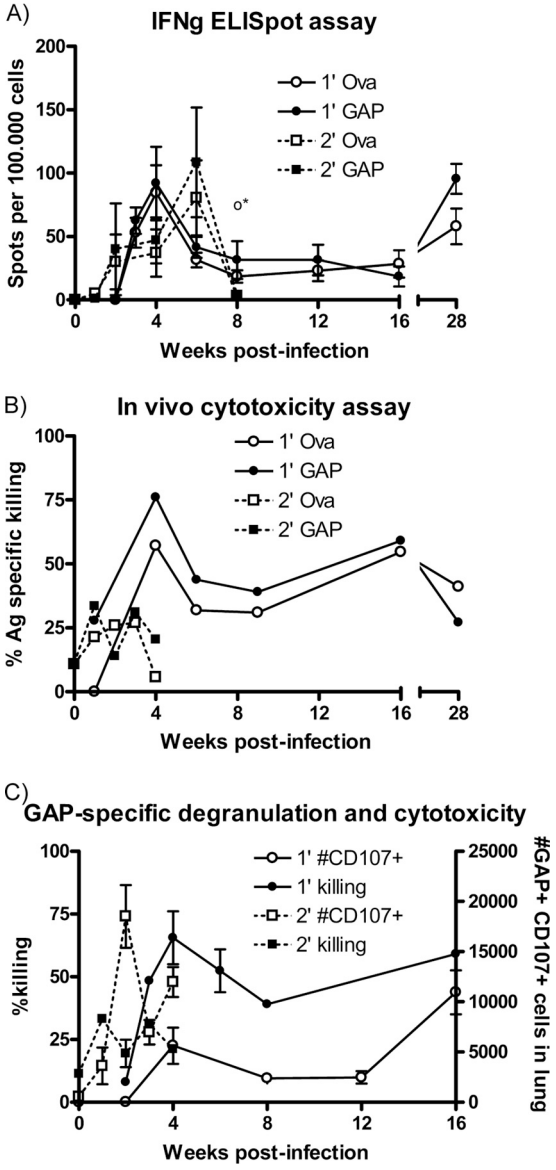

FIG. 4. Functional assays for GAP- and OVA-specific cytotoxicity and IFN-γ secretion. (A) ELISPOT assay, where lung cells were incubated with DCs pulsed with GAP or OVA peptide (SIINFEKL) for 48 h. There was no background level of IFN-γ (IFNg) secretion, measured by incubating cells with either T-cell media or unpulsed, uninfected DCs (data not shown). Data are means ± standard errors of the means from test results for four mice per time point. There was no statistical significance between primary (1′) and secondary (2′) infections, except for OVA-specific cells at 8 weeks postinfection ($P < 0.05$). (B) In vivo cytotoxicity assay in the lung. Data are the averages from test results using four mice per group. (C) GAP-specific cytotoxicity versus the frequency of $CD107^+$ GAP-specific CD8 T cells in the lung. There was a significant correlation ($P < 0.05$) between cytotoxicity and CD107 surface expression during primary infection, as measured by the Spearman nonparametric test, while there was not a significant correlation during secondary infection.

memory and primary T cells, since bacteria are not cleared, allowing for priming of new T cells.

GAP- and OVA-specific memory CD8 T-cell expansion was significantly larger than primary CD8 T-cell expansion in response to these epitopes in terms of the number of cells ($P < 0.01$) (Fig. 2A and B), and they represented a greater proportion of the total CD8 T-cell response ($P < 0.01$ for OVA; $P < 0.05$ for GAP) (see Fig. S1 in the supplemental material). This indicates that GAP and OVA CD8 T-cell epitopes are presented during both primary and secondary infections. Memory T-cell expansion against *M. tuberculosis* was associated with an earlier control of bacterial numbers in the lung ($P < 0.01$) (Fig. 2C). This protection was transient, as previously published (18), indicating that memory CD8 T cells induced by infection in this model do not confer significant long-term protection against subsequent *M. tuberculosis* infection. *M. tuberculosis*-specific CD8 T cells did not contract despite control of bacterial infection, reaching higher numbers in the lung than during primary infection (Fig. 2A). Masopust et al. showed, using heterologous infections, that cells contracted more slowly with each subsequent infection (30). Based on this, chronic antigen exposure during *M. tuberculosis* infection may cause the slow contraction of cells.

In summary, both GAP and OVA memory CD8 T cells are present in the lungs at higher levels during *M. tuberculosis* reinfection, indicating a more rapid and robust response to secondary challenge.

Function of CD8 T cells specific for GAP and OVA during rechallenge with *M. tuberculosis* strain ova. Before reinfection of mice, residual *M. tuberculosis*-specific CD8 T cells in the lungs had a cytotoxic phenotype ($CD107^+$) (Fig. 3C and D; see also Fig. S3C and D and S4C and D in the supplemental material). There was a continued expansion of $CD107^+$ cells in the lungs following reinfection. IFN-γ-secreting cells appeared by 2 weeks postinfection, as measured by ELISPOT assay (Fig. 4A). As in primary infection, almost no cells were observed that both secreted IFN-γ and degranulated (Fig. 3C and D; see also Fig. S3C and D and S4C and D in the supplemental material). By 3 weeks postinfection, CD8 T cells expressing IFN-γ were observed by flow cytometry. These cells are presumably newly primed, since they correspond to the peak of these cells in primary infection. After 3 weeks postinfection, cytotoxicity, as measured by the in vivo cytotoxicity assay, decreased (Fig. 4B), despite continued expansion of $CD107^+$ cells (Fig. 3C and D). The lack of correlation between GAP-specific cytotoxicity and the frequency of $CD107^+$ GAP-specific cells in the lungs (Fig. 4C), unlike what was observed during primary infection, suggests that although memory CD8 T cells are capable of degranulation, they are less efficient at killing targets during secondary infection.

To summarize, cytotoxicity is the main function of *M. tuberculosis*-specific memory CD8 T cells in the lungs and appears to be the main function of primary CD8 T-cell responses. By 4 weeks postinfection, however, the memory CD8 T-cell response was altered compared to primary responses, in that cytotoxicity had decreased.

Cytotoxic effector molecules. To address a potential cause of decreased cytotoxicity during secondary infection, we examined expression of perforin and granzyme B (see Fig. S2I in the supplemental material). They are the primary cytotoxic effector molecules, stored in lytic vesicles, during *M. tuberculosis* infection (39). While granzyme B protein levels were low in both primary and memory GAP-specific CD8 T cells in unstimulated samples (Fig. 6A), incubation with anti-CD3 and

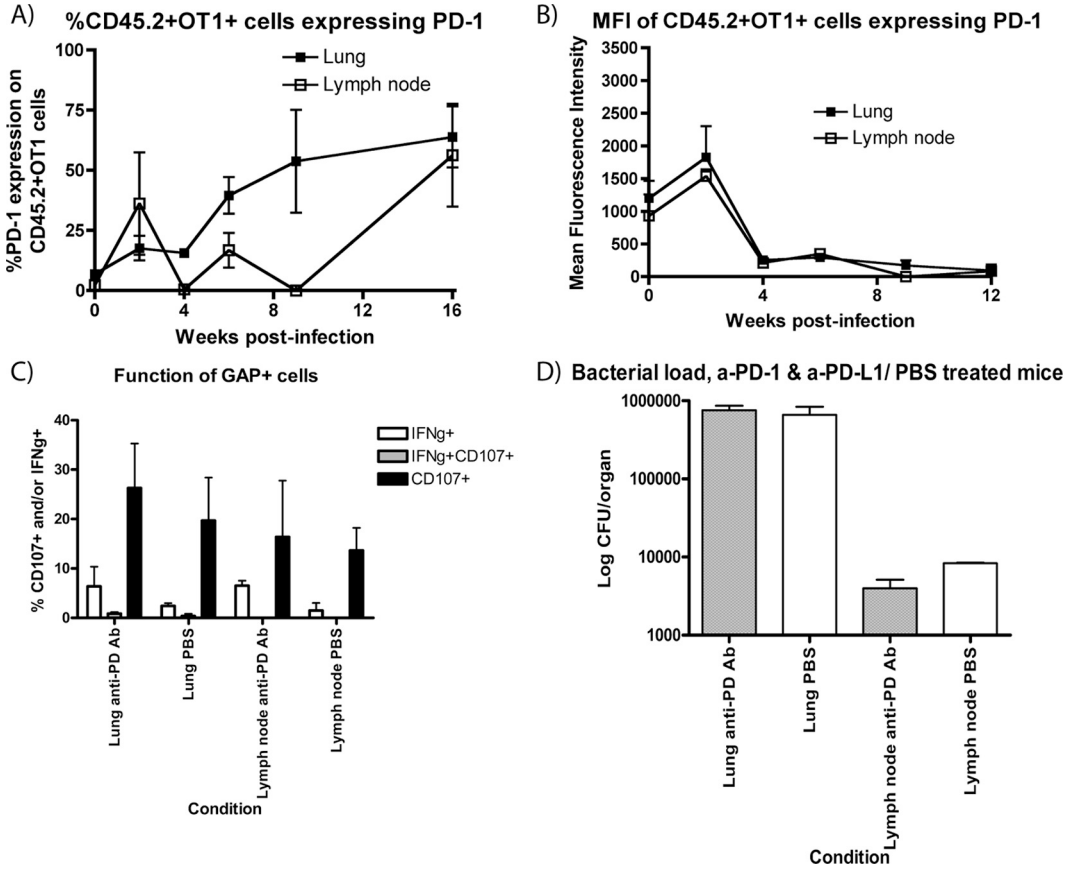

FIG. 5. Blocking PD-1 signal in vivo does not give IFN-γ^+ CD107$^+$ cells. A total of 5×10^3 OT-I cells (CD45.2) were adoptively transferred to CD45.1 mice, which were subsequently infected with *M. tuberculosis* strain ova. Using anti-CD45.2 antibodies, responses of these cells were examined over the course of infection. (A) Percent CD45.2$^+$ OT-I$^+$ cells expressing PD-1; (B) geometric MFI of PD-1 staining in panel A. (C and D) Mice treated with anti-PD-1 and anti-PD-L1 antibodies, or with PBS, for 4 weeks. Ab, antibody; a-, anti-. (C) GAP$^+$ CD8 T cells expressing IFN-γ (IFNg) and surface CD107. (D) Bacterial load in the lung and lymph nodes. Data are the means ± standard errors of the means from test results for three or four mice per experimental group.

anti-CD28 antibodies could increase expression in both primary and memory cells ($P < 0.05$ at weeks 2 and 6 postinfection) (Fig. 6B). Perforin levels, on the other hand, were high in both primary and secondary unstimulated GAP-specific CD8 T cells (Fig. 6A).

Both primary and memory GAP-specific CD8 T cells had high levels of perforin, while granzyme B could be induced in both. Thus, a lack of effector molecules in recalled CD8 T cells is unlikely to account for the reduction in actual cytotoxicity during the later memory response.

Degranulation and IFN-γ secretion are highest in IFN-γ^+ CD107$^+$ cells. Although IFN-γ^+ CD107$^+$ cells were a very small population during primary infection, these cells produced the most IFN-γ, as determined by flow cytometry using geometric MFI (IFN-γ^+ CD107$^+$ versus IFN-γ^+ CD107$^-$ cells at 4 weeks postinfection; $P < 0.05$) (Fig. 7A). The quantity of IFN-γ secreted on a per-cell basis decreased during secondary infection (IFN-γ^+ CD107$^+$ cells at 4 weeks postinfection; primary versus secondary responses; $P < 0.05$) (Fig. 7A; see also Fig. S2B and C in the supplemental material), while the frequency of secreting cells was slightly increased (4 weeks postinfection; primary versus secondary responses; $P < 0.05$) (Fig. 3A and B).

During primary infection, CD107 MFI remained constant, and there was little difference between CD107$^+$ and IFN-γ^+ CD107$^+$ cells until late in the infection, when there was increased degranulation, especially by IFN-γ^+ CD107$^+$ cells (Fig. 7B). Both numbers (4 weeks postinfection; primary versus secondary responses; $P < 0.01$) (Fig. 3A and B) and the MFI ($P < 0.01$) (Fig. 7B; see also Fig. S2E and F in the supplemental material) of degranulating cells were higher during secondary infection, while actual cytotoxicity, as measured in an in vivo assay, was decreased compared to that during primary infection (Fig. 4B and C).

In summary, IFN-γ^+ CD107$^+$ cells may be the best effector cells, although they were very small populations and their contribution to the control of *M. tuberculosis* was small, while less efficient cells constituted the bulk of the response.

DISCUSSION

In this study, we characterized the multifunctional nature of *M. tuberculosis*-specific CD8 T-cell responses in the murine model. Using a recombinant strain expressing OVA epitopes (*M. tuberculosis* strain ova), OVA-specific CD8 T-cell responses were shown to be comparable to CD8 T-cell responses

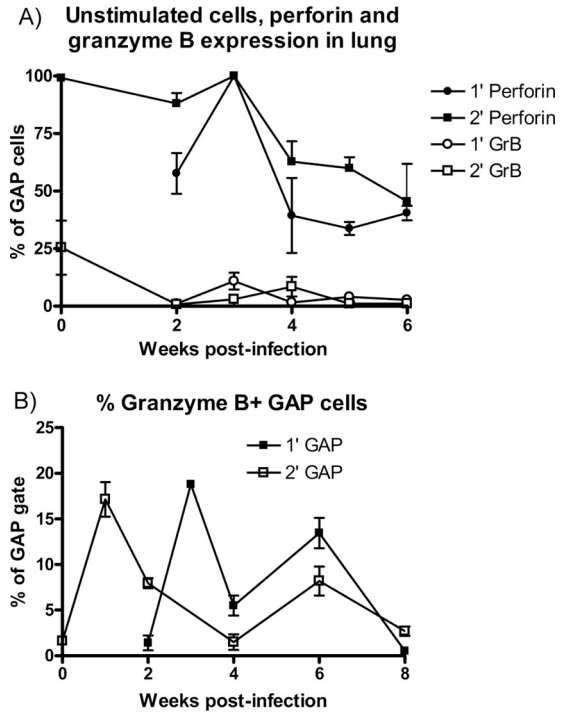

FIG. 6. CD8 T cells express perforin, while granzyme B expression can be induced. (A) Cells were stained, without incubation, for perforin (fluorescein isothiocyanate, clone dG9) and granzyme B (GrB), using fixative and a protocol from Apo-Active 3 (Cell Technology, Mountain View, CA). 1′, primary infection; 2′, secondary infection. (B) Cells were stained for granzyme B after a 5-h incubation, as described in Materials and Methods. Data are the means ± standard errors of the means from test results for three or four mice per experimental group.

to an endogenous *M. tuberculosis* epitope (GAP) over the course of both primary and secondary infections in C57BL/6 mice. *M. tuberculosis* strain ova persistence in the host is comparable to that of the WT strain, despite the addition of a CD8 T-cell epitope to CFP10. The GAP- and OVA-specific CD8 T-cell responses are comparable to, albeit smaller than, those seen against *M. tuberculosis*-specific CD8 T-cell epitopes, such as TB10.3/4 (6, 17). There has been a lack of good reagents to study CD8 T-cell responses in C57BL/6 mice, even though it is the most commonly used mouse strain in tuberculosis research. Advances in the use of tetramers and new assays for function of CD8 T cells, as well as the use of the recombinant *M. tuberculosis* strain ova and OVA-specific reagents, will allow for more in-depth studies of CD8 T-cell responses in tuberculosis.

IFN-γ secretion and cytotoxic function have been traditional measurements of CD8 T-cell responses. Study of CD8 T-cell responses to *M. tuberculosis* infection has been complicated by the fact that CD8 T cells are a minor contributor of IFN-γ compared to CD4 T cells (9; our unpublished results), and until recently, in vitro expansion of *M. tuberculosis*-specific CD8 T cells was required to measure cytotoxic function (24). In other systems, it has been reported that induction of IFN-γ secretion requires more antigen than cytotoxicity (35). While *M. tuberculosis* expansion is contained by 4 weeks postinfection, we previously showed that antigen accumulates in the lungs as the infection progresses (24). This indicates that the lack of antigen exposure is likely not the cause of the low number of IFN-γ-secreting CD8 T cells. This is supported by the finding that coincubation in an ELISPOT assay with antigen-pulsed DCs was not sufficient to induce IFN-γ secretion from CD8 T cells after the peak of infection at 4 weeks (Fig. 4A). It is possible that IFN-γ-secreting cells contracted, leaving cells primed for other functions, that cells with different functions entered the lungs, or that IFN-γ secretion was blocked. This block may be relieved as bacterial infection is cleared by antibiotics, as memory cells could respond by making IFN-γ, although the per-cell amount was reduced compared to that produced during primary infection (Fig. 7A).

Studies examining CD8 T-cell-mediated cytotoxicity in tuberculosis have generated conflicting results. Previous work from our laboratory, using in vitro cultured cells from C57BL/6 mice to assay for cytotoxicity, indicated that CD8 T cells lost cytotoxic function by 4 weeks postinfection (24). Work by Kamath et al., using an in vivo cytotoxicity assay with BALB/c mice, indicates that CD8 T cells retain their cytotoxic function throughout infection (19). It is likely that in vitro culture of cells led us to underestimate the frequency of cytotoxic CD8 T

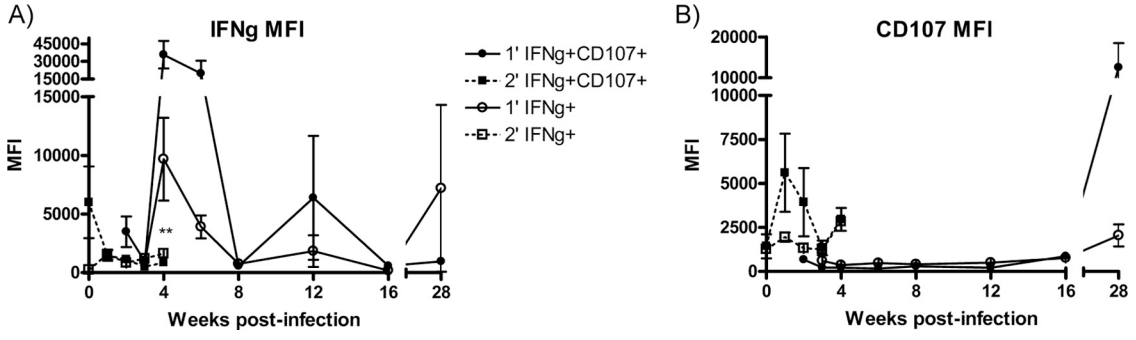

FIG. 7. IFN-γ^+ CD107$^+$ cells secrete more IFN-γ and degranulate more than cells limited to either function. The geometric MFIs of CD107$^+$ and IFN-γ^+ GAP-specific cells were analyzed. IFN-γ (IFNg) MFI (A) or CD107 MFI (B) of cells that both secrete IFN-γ and degranulate or are limited to either function. Data are the means ± standard errors of the means from test results for four mice per time point. There were significant differences in both IFN-γ secretion and degranulation between primary (1′) and secondary (2′) infections ($P < 0.05$) at 3 and 4 weeks postinfection. IFN-γ^+ CD107$^+$ cells expressed significantly more IFN-γ at 4 weeks postinfection than IFN-γ^+ CD107$^-$ cells ($P < 0.01$), while there was no significant difference in degranulation between IFN-γ^+ CD107$^+$ and IFN-γ^- CD107$^+$ cells.

cells in infected lungs, as cells from the lungs can be highly activated (33) and prone to apoptosis in vitro. Recent work by Billeskov et al. (6), using the in vivo cytotoxicity assay with C57BL/6 mice, indicated that cytotoxicity peaks at 4 weeks postinfection and decreases slightly with time. We observed decreased cytotoxicity after 4 weeks, tracking a different CD8 T-cell population, followed by an increase late in primary infection as the frequency of degranulating cells increased. The frequency of cells expressing surface CD107 correlated well with cytotoxicity during primary infection but not during secondary infection, where cytotoxicity was decreased compared to that during primary infection, despite an increase in the frequency of degranulating cells. Wolint et al. (38) showed that cytotoxicity by memory cells was related to effector molecules in lytic granules rather than degranulation. Partial CD8 T-cell exhaustion caused by a lack of effector molecules may be the cause of decreased cytotoxicity during secondary *M. tuberculosis* infection, although the cells expressed perforin, and granzyme B expression could be induced by antigen stimulation. It is possible that antigen-pulsed targets used for in vivo cytotoxicity assays did not stimulate the cells sufficiently to induce granzyme B expression.

An unexpected finding was that, on a single-cell basis, the vast majority of CD8 T cells induced by infection with *M. tuberculosis* were not capable of both secreting IFN-γ and degranulating. This contrasts with data from other chronic infections, such as human immunodeficiency virus type 1, where CD8 T cells chronically exposed to antigen are able to perform both functions (10). During chronic LCMV infection, cells appear to be primarily cytotoxic, while CD8 T cells from acutely infected mice retain the ability to both be cytotoxic and secrete IFN-γ (1). Presumably, the phenotype of cytotoxicity only is due to constant antigen exposure during chronic LCMV infection, leading to exhaustion of the CD8 T cells. However, it is unlikely that distinct $CD107^+$ and IFN-γ^+ cell populations that arise during the initial phase of *M. tuberculosis* infection are due to exhaustion from chronic antigen exposure, as the inoculum is low and the bacterium slow growing, while the functional division, i.e., IFN-γ secretion or degranulation, is maintained from the initial priming events of the adaptive immune response. Additionally, while the frequency of cells expressing PD-1 increased over the course of *M. tuberculosis* infection, which has been correlated to CD8 T-cell exhaustion in other infections (3, 31), the expression levels decreased following priming, and administration of blocking antibodies for 4 weeks had no significant effect on CD8 T-cell function or the bacterial load (Fig. 5).

In summary, *M. tuberculosis* infection yielded CD8 T cells that were, to a large extent, unable to both be cytotoxic and secrete IFN-γ and memory responses that were less functional than primary responses. Elucidating the cause of the poor quality of CD8 T-cell responses may enable the generation of improved vaccines against *M. tuberculosis*.

ACKNOWLEDGMENTS

This work was supported by NIH/NIAID grants 2RO1 AI37859-11 and NO1 AI50018.

We thank Gordon J. Freeman for providing the anti-PD-1 and anti-PD-L1 antibodies. We thank Hillarie P. Windish and Angela M. Green for discussions and technical assistance and Elisabet Einarsdottir for critical reading of the manuscript.

REFERENCES

1. **Agnellini, P., P. Wolint, M. Rehr, J. Cahenzli, U. Karrer, and A. Oxenius.** 2007. Impaired NFAT nuclear translocation results in split exhaustion of virus-specific CD8+ T cell functions during chronic viral infection. Proc. Natl. Acad. Sci. USA **104:**4565–4570.
2. **Algood, H. M. S., P. L. Lin, D. Yankura, A. Jones, J. Chan, and J. L. Flynn.** 2004. TNF influences chemokine expression of macrophages in vitro and that of CD11b+ cells in vivo during Mycobacterium tuberculosis infection. J. Immunol. **172:**6846–6857.
3. **Barber, D. L., E. J. Wherry, D. Masopust, B. Zhu, J. P. Allison, A. H. Sharpe, G. J. Freeman, and R. Ahmed.** 2006. Restoring function in exhausted CD8 T cells during chronic viral infection. Nature **439:**682–687.
4. **Betts, M. R., J. M. Brenchley, D. A. Price, S. C. De Rosa, D. C. Douek, M. Roederer, and R. A. Koup.** 2003. Sensitive and viable identification of antigen-specific CD8+ T cells by a flow cytometric assay for degranulation. J. Immunol. Methods **281:**65–78.
5. **Bibb, L. A., and G. F. Hatfull.** 2002. Integration and excision of the Mycobacterium tuberculosis prophage-like element, phiRv1. Mol. Microbiol. **45:** 1515–1526.
6. **Billeskov, R., C. Vingsbo-Lundberg, P. Andersen, and J. Dietrich.** 2007. Induction of CD8 T cells against a novel epitope in TB10.4: correlation with mycobacterial virulence and the presence of a functional region of difference-1. J. Immunol. **179:**3973–3981.
7. **Chege, G., R. Warren, N. van Pittius, W. Burgers, R. Wilkinson, E. Shephard, and A.-L. Williamson.** 2008. Detection of natural infection with Mycobacterium intracellulare in healthy wild-caught Chacma baboons (Papio ursinus) by ESAT-6 and CFP-10 IFN-gamma ELISPOT tests following a tuberculosis outbreak. BMC Microbiol. **8:**27.
8. **Cosma, C. L., O. Humbert, and L. Ramakrishnan.** 2004. Superinfecting mycobacteria home to established tuberculous granulomas. Nat. Immunol. **5:**828–835.
9. **Cowley, S. C., and K. L. Elkins.** 2003. CD4+ T cells mediate IFN-γ-independent control of Mycobacterium tuberculosis infection both in vitro and in vivo. J. Immunol. **171:**4689–4699.
10. **Critchfield, J. W., D. Lemongello, D. H. Walker, J. C. Garcia, D. M. Asmuth, R. B. Pollard, and B. L. Shacklett.** 2007. Multifunctional human immunodeficiency virus (HIV) Gag-specific $CD8^+$ T-cell responses in rectal mucosa and peripheral blood mononuclear cells during chronic HIV type 1 infection. J. Virol. **81:**5460–5471.
11. **Day, C. L., D. E. Kaufmann, P. Kiepiela, J. A. Brown, E. S. Moodley, S. Reddy, E. W. Mackey, J. D. Miller, A. J. Leslie, C. DePierres, Z. Mncube, J. Duraiswamy, B. Zhu, Q. Eichbaum, M. Altfeld, E. J. Wherry, H. M. Coovadia, P. J. R. Goulder, P. Klenerman, R. Ahmed, G. J. Freeman, and B. D. Walker.** 2006. PD-1 expression on HIV-specific T cells is associated with T-cell exhaustion and disease progression. Nature **443:**350–354.
12. **Flynn, J. L., and J. Chan.** 2001. Immunology of tuberculosis. Annu. Rev. Immunol. **19:**93–129.
13. **Gao, W., A. Rzewski, H. Sun, P. D. Robbins, and A. Gambotto.** 2004. UpGene: application of a web-based DNA codon optimization algorithm. Biotechnol. Prog. **20:**443–448.
14. **Gutzmer, R., W. Li, S. Sutterwala, M. P. Lemos, J. I. Elizalde, S. L. Urtishak, E. M. Behrens, P. M. Rivers, K. Schlienger, T. M. Laufer, S. L. Eck, and M. S. Marks.** 2004. A tumor-associated glycoprotein that blocks MHC class II-dependent antigen presentation by dendritic cells. J. Immunol. **173:**1023–1032.
15. **Irwin, S. M., A. A. Izzo, S. W. Dow, Y. A. W. Skeiky, S. G. Reed, M. R. Alderson, and I. M. Orme.** 2005. Tracking antigen-specific CD8 T lymphocytes in the lungs of mice vaccinated with the Mtb72F polyprotein. Infect. Immun. **73:**5809–5816.
16. **Jeon, B. Y., S. C. Derrick, J. Lim, K. Kolibab, V. Dheenadhayalan, A. L. Yang, B. Kreiswirth, and S. L. Morris.** 2008. *Mycobacterium bovis* BCG immunization induces protective immunity against nine different *Mycobacterium tuberculosis* strains in mice. Infect. Immun. **76:**5173–5180.
17. **Kamath, A., J. S. M. Woodworth, and S. M. Behar.** 2006. Antigen-specific CD8+ T cells and the development of central memory during Mycobacterium tuberculosis infection. J. Immunol. **177:**6361–6369.
18. **Kamath, A. B., and S. M. Behar.** 2005. Anamnestic responses of mice following *Mycobacterium tuberculosis* infection. Infect. Immun. **73:**6110–6118.
19. **Kamath, A. B., J. Woodworth, X. Xiong, C. Taylor, Y. Weng, and S. M. Behar.** 2004. Cytolytic CD8+ T cells recognizing CFP10 are recruited to the lung after Mycobacterium tuberculosis infection. J. Exp. Med. **200:**1479–1489.
20. **Karlsson, A. C., J. N. Martin, S. R. Younger, B. M. Bredt, L. Epling, R. Ronquillo, A. Varma, S. G. Deeks, J. M. McCune, D. F. Nixon, and E. Sinclair.** 2003. Comparison of the ELISPOT and cytokine flow cytometry assays for the enumeration of antigen-specific T cells. J. Immunol. Methods **283:**141–153.
21. **Keane, J., M. K. Balcewicz-Sablinska, H. G. Remold, G. L. Chupp, B. B. Meek, M. J. Fenton, and H. Kornfeld.** 1997. Infection by *Mycobacterium tuberculosis* promotes human alveolar macrophage apoptosis. Infect. Immun. **65:**298–304.

22. **Khan, I. H., R. Ravindran, J. Yee, M. Ziman, D. M. Lewinsohn, M. L. Gennaro, J. L. Flynn, C. W. Goulding, K. DeRiemer, N. W. Lerche, and P. A. Luciw.** 2008. Profiling antibodies to *Mycobacterium tuberculosis* by multiplex microbead suspension arrays for serodiagnosis of tuberculosis. Clin. Vaccine Immunol. **15:**433–438.
23. **Larsen, M. H.** 2000. Some common methods in mycobacterial genetics, p. 313–320. *In* G. F. Hatfull and W. R. Jacobs (ed.), Molecular genetics of mycobacteria. ASM Press, Washington, DC.
24. **Lazarevic, V., D. Nolt, and J. L. Flynn.** 2005. Long-term control of Mycobacterium tuberculosis infection is mediated by dynamic immune responses. J. Immunol. **175:**1107–1117.
25. **Lee, M. H., L. Pascopella, W. R. Jacobs, Jr., and G. F. Hatfull.** 1991. Site-specific integration of mycobacteriophage L5: integration-proficient vectors for Mycobacterium smegmatis, Mycobacterium tuberculosis, and bacille Calmette-Guerin. Proc. Natl. Acad. Sci. USA **88:**3111–3115.
26. **Lewinsohn, D. M., L. Zhu, V. J. Madison, D. C. Dillon, S. P. Fling, S. G. Reed, K. H. Grabstein, and M. R. Alderson.** 2001. Classically restricted human CD8+ T lymphocytes derived from Mycobacterium tuberculosis-infected cells: definition of antigenic specificity. J. Immunol. **166:**439–446.
27. **Lightbody, K. L., P. S. Renshaw, M. L. Collins, R. L. Wright, D. M. Hunt, S. V. Gordon, R. G. Hewinson, R. S. Buxton, R. A. Williamson, and M. D. Carr.** 2004. Characterisation of complex formation between members of the Mycobacterium tuberculosis complex CFP-10/ESAT-6 protein family: towards an understanding of the rules governing complex formation and thereby functional flexibility. FEMS Microbiol. Lett. **238:**255–262.
28. **Majlessi, L., M.-J. Rojas, P. Brodin, and C. Leclerc.** 2003. $CD8^+$ T-cell responses of mycobacterium-infected mice to a newly identified major histocompatibility complex class I-restricted epitope shared by proteins of the ESAT-6 family. Infect. Immun. **71:**7173–7177.
29. **Martin, A., M. Herranz, M. Serrano, E. Bouza, and D. de Viedma.** 2007. Rapid clonal analysis of recurrent tuberculosis by direct MIRU-VNTR typing on stored isolates. BMC Microbiol. **7:**73.
30. **Masopust, D., S.-J. Ha, V. Vezys, and R. Ahmed.** 2006. Stimulation history dictates memory CD8 T cell phenotype: implications for prime-boost vaccination. J. Immunol. **177:**831–839.
31. **Petrovas, C., J. P. Casazza, J. M. Brenchley, D. A. Price, E. Gostick, W. C. Adams, M. L. Precopio, T. Schacker, M. Roederer, D. C. Douek, and R. A. Koup.** 2006. PD-1 is a regulator of virus-specific CD8+ T cell survival in HIV infection. J. Exp. Med. **203:**2281–2292.
32. **Serbina, N. V., and J. L. Flynn.** 2001. $CD8^+$ T cells participate in the memory immune response to *Mycobacterium tuberculosis*. Infect. Immun. **69:**4320–4328.
33. **Serbina, N. V., C.-C. Liu, C. A. Scanga, and J. L. Flynn.** 2000. CD8+ CTL from lungs of Mycobacterium tuberculosis-infected mice express perforin in vivo and lyse infected macrophages. J. Immunol. **165:**353–363.
34. **Urbani, S., B. Amadei, D. Tola, M. Massari, S. Schivazappa, G. Missale, and C. Ferrari.** 2006. PD-1 expression in acute hepatitis C virus (HCV) infection is associated with HCV-specific CD8 exhaustion. J. Virol. **80:**11398–11403.
35. **Valitutti, S., S. Muller, M. Dessing, and A. Lanzavecchia.** 1996. Different responses are elicited in cytotoxic T lymphocytes by different levels of T cell receptor occupancy. J. Exp. Med. **183:**1917–1921.
36. **Verver, S., R. M. Warren, N. Beyers, M. Richardson, G. D. van der Spuy, M. W. Borgdorff, D. A. Enarson, M. A. Behr, and P. D. van Helden.** 2005. Rate of reinfection tuberculosis after successful treatment is higher than rate of new tuberculosis. Am. J. Respir. Crit. Care Med. **171:**1430–1435.
37. **Warren, R. M., T. C. Victor, E. M. Streicher, M. Richardson, N. Beyers, N. C. G. van Pittius, and P. D. van Helden.** 2004. Patients with active tuberculosis often have different strains in the same sputum specimen. Am. J. Respir. Crit. Care Med. **169:**610–614.
38. **Wolint, P., M. R. Betts, R. A. Koup, and A. Oxenius.** 2004. Immediate cytotoxicity but not degranulation distinguishes effector and memory subsets of CD8+ T cells. J. Exp. Med. **199:**925–936.
39. **Woodworth, J. S., Y. Wu, and S. M. Behar.** 2008. Mycobacterium tuberculosis-specific CD8+ T cells require perforin to kill target cells and provide protection in vivo. J. Immunol. **181:**8595–8603.

Editor: R. P. Morrison